First-Principles Calculations of the Adsorption of Nitromethane and 1,1-Diamino-2,2-dinitroethylene (FOX-7) Molecules on the Al(111) Surface

Dan C. Sorescu,*,† Jerry A. Boatz,*,‡ and Donald L. Thompson*,§

U.S. Department of Energy, National Energy Technology Laboratory, P.O. Box 10940, Pittsburgh, Pennsylvania 15236, Department of Chemical and Petroleum Engineering, University of Pittsburgh, Pittsburgh, Pennsylvania 15260, Air Force Research Laboratory, AFRL/PRSP, Edwards Air Force Base, California 93524, and Department of Chemistry, Oklahoma State University, Stillwater, Oklahoma 74078

First-principles calculations that are based on spin-unrestricted density functional theory and the generalized gradient approximation have been used to study the adsorption of nitromethane and 1,1-diamino-2,2-dinitroethylene molecules on the Al(111) surface. The calculations employ (3×3) aluminum slab geometries and three-dimensional periodic boundary conditions. On the basis of these calculations, we have determined that both dissociative and nondissociative adsorption mechanisms are possible, depending on the molecular orientation and the particular surface sites involved. In the case of dissociative chemisorption, O-atom abstraction by Al surface atoms has been determined to be the dominant mechanism. The dissociated O atom forms strong Al−O bonds with the neighboring Al sites around the dissociation sites. In addition, the radical species obtained as a result of O-atom elimination remains bonded to the surface. In some instances, both O atoms of the nitro group dissociate and oxidize the aluminum surface. Finally, for the case of nondissociative adsorption, various N−O−Al bridge-type bonding configurations can be formed. On the basis of the data provided from these studies, it can be concluded that oxidation of the aluminum surface readily occurs, either by partial or complete dissociation of the O atoms from the NO_2 group.

I. Introduction

Powderized aluminum has long been used as an energetic ingredient in rocket propellant formulations, comprising ~15%−20% of conventional ammonium perchlorate solid propellant.[1] Its primary roles are to (i) increase the combustion exothermicity, (ii) increase the regression rate of solid propellant grains, and (iii) enhance the blasting effect of explosives. Such properties are significantly affected by the size of the aluminum particles. For example, in the case of aluminum nanopowders, significant improvements in the performance of some energetic materials over common micrometer-size aluminum powders have been reported.[2,3]

An important performance issue, particularly for nanoscale aluminum powders, is the formation of an aluminum oxide overcoat prior to combustion, which inhibits efficient burning. When the thickness of the oxide overcoat is large, its presence severely reduces the potential advantages of using ultrafine aluminum particles with such a high surface-area-to-volume ratio. Consequently, identification of new methods for the passivation of aluminum particles to reduce the size of the oxide layer, without incurring a significant decrease in performance, is being considered. Furthermore, aluminum is commonly used in formulations of propellants and explosives,[4] and it is important to understand its reactions with energetic molecules.

Currently, no experimental evidence is available to clarify the efficiency of passivation of aluminum nanoparticles when coated with various energetic materials. Moreover, a clear mechanism to describe the interaction of energetic materials (nitro compounds in particular) with aluminum surfaces is lacking. To clarify some of the fundamental issues related to the role of energetic materials when deposited on an aluminum surface, the present work focuses on the atomic-level description of the interactions between the energetic compounds nitromethane (NM) and 1,1-diamino-2,2-dinitroethylene (FOX-7) with the Al(111) surface. Specifically, first-principles quantum chemical calculations are used to determine the chemisorption properties of the nitro-containing compounds of interest for energetic materials applications on aluminum surfaces.

II. Computational Method

The calculations performed in this study were done using the VASP package.[5−7] This program evaluates the total energy of periodically repeating geometries, on the basis of density functional theory (DFT) and the pseudo-potential approximation. The electron−ion interaction is described by fully nonlocal optimized ultrasoft pseudo-potentials that are similar to those introduced by Vanderbilt.[8,9] Periodic boundary conditions are used, with the one-electron pseudo-orbitals expanded over a plane-wave basis set. The expansion includes all plane waves whose kinetic energy is defined as $\hbar^2k^2/2m < E_{cut}$, where k is the wave vector, m the electronic mass, and E_{cut} the chosen cutoff energy. In this study, a cutoff energy of 395 eV is chosen, which ensures the convergence with respect to the basis set. Several tests to probe the convergence characteristics are provided in the next section.

Calculations were performed using spin-unrestricted generalized gradient approximation (GGA) density functional theory, which used the PW91 exchange-correlation functional.[10] Sam-

* Author to whom correspondence should be addressed. E-mail: dlt@okstate.edu.
† National Energy Technology Laboratory and University of Pittsburgh.
‡ Air Force Research Laboratory.
§ Oklahoma State University.

pling of the Brillouin zone was performed using a Monkhorst−Pack scheme.[11] We have also used the Methfessel−Paxton technique[12] with a smearing of $\sigma = 0.2$ eV, to minimize the errors in the Hellmann−Feynman forces due to the entropic contribution to the electronic free energy.[5,6] All energies are extrapolated to a temperature of $T = 0$ K.

The minimization of the electronic free energy was performed using an efficient iterative matrix-diagonalization routine that was based on a sequential band-by-band residuum minimization method (RMM)[5,6] or was alternatively based on preconditioned band-by-band conjugate-gradient (CG) minimization.[13] The optimization of different atomic configurations was performed by CG minimization of the total energy.

The aluminum surface is represented by a slab model with periodic boundary conditions applied in all three directions. Particularly, a 3×3 supercell with four layers containing 36 Al atoms is used to study the adsorption of various molecular systems (see Figure 1). The slabs were separated by 10 and 15 Å of vacuum for the cases of the NM and FOX-7 molecules, respectively. In calculations of molecular adsorption on the surface, we have relaxed all atomic positions of the molecule, as well as the Al atoms located in the first layer of the slab.

III. Results and Discussion

A. Test Calculations for Bulk Aluminum and Isolated NM and FOX-7 Molecules. Several tests have been initially performed to verify the accuracy of the method when applied to bulk aluminum and to the isolated NM and FOX-7 molecules, as well as to clarify different technical aspects, such as the optimum cutoff energy for calculations.

For bulk aluminum, we have tested for convergence, using the *k*-point sampling density and the kinetic energy cutoff. In these calculations, a Monkhorst−Pack scheme[11] with mesh parameters of $12 \times 12 \times 12$ has been used, leading to 56 *k*-points in the irreducible Brillouin zone. To determine the equilibrium bulk parameters of aluminum, we have uniformly scaled the lattice vectors and performed energy calculations as a function of the unit-cell volume. The calculated data were then fit with the Murnaghan equation of state.[14] The calculated lattice constant varies from 4.047 Å at $E_{cut} = 161.5$ eV, to 4.044 Å at $E_{cut} = 395$ eV and 4.044 Å at $E_{cut} = 495$ eV. It can be concluded that, at $E_{cut} = 395$ eV, the bulk structure is well converged, with respect to the cutoff energy. The calculated lattice constant of 4.044 Å is also in very good agreement with the experimental value of 4.050 Å,[15] with a relative difference of only −0.14%. The corresponding bulk modulus and its pressure derivative were $B_0 = 72.2$ GPa and $B_0' = 4.16$, respectively. These values respectively differ by −4.87% and −2.57% from the corresponding values of 75.9 GPa and 4.27, which were estimated in the work of Gaudoin and Foulkes[16] on the basis of the reported elastic constants of aluminum. These values indicate that the present set of pseudo-potentials is able to provide a very good representation of the structural properties of bulk aluminum.

An equally good representation has been observed for the geometric parameters of the isolated NM and FOX-7 molecules. For example, on the basis of optimizations of the isolated NM molecule in a cubic box with dimensions of 12 Å × 12 Å × 12 Å, we have determined the following: equilibrium bond lengths of r(C−N) = 1.497 Å, r(N−O) = 1.240 Å, and r(C−H) = 1.090 Å, and bond angles of θ(N−C−H) = 106.6° and θ(N−O−N) = 125.6° at $E_{cut} = 396$ eV. The increase of the cutoff energy to 495 eV leads to the following values: r(C−N) = 1.496 Å, r(N−O) = 1.240 Å, r(C−H) = 1.091 Å, θ(N−C−H) = 107.6°, and θ(N−O−N) = 125.6°. We notice that there are no significant differences between the values obtained at the two cutoff energies, indicating convergence of the results even at $E_{cut} = 395$ eV. These values are also very similar to those that we have reported previously[17] for the isolated NM molecule, on the basis of hybrid DFT calculations at the B3LYP/6-31G** theoretical level. In addition, the calculated values are also similar to the experimental data for gas-phase NM.[18] In this case, the largest deviation—0.016 Å—is observed for N−O bonds (r^{exp}(N−O) = 1.224 Å).

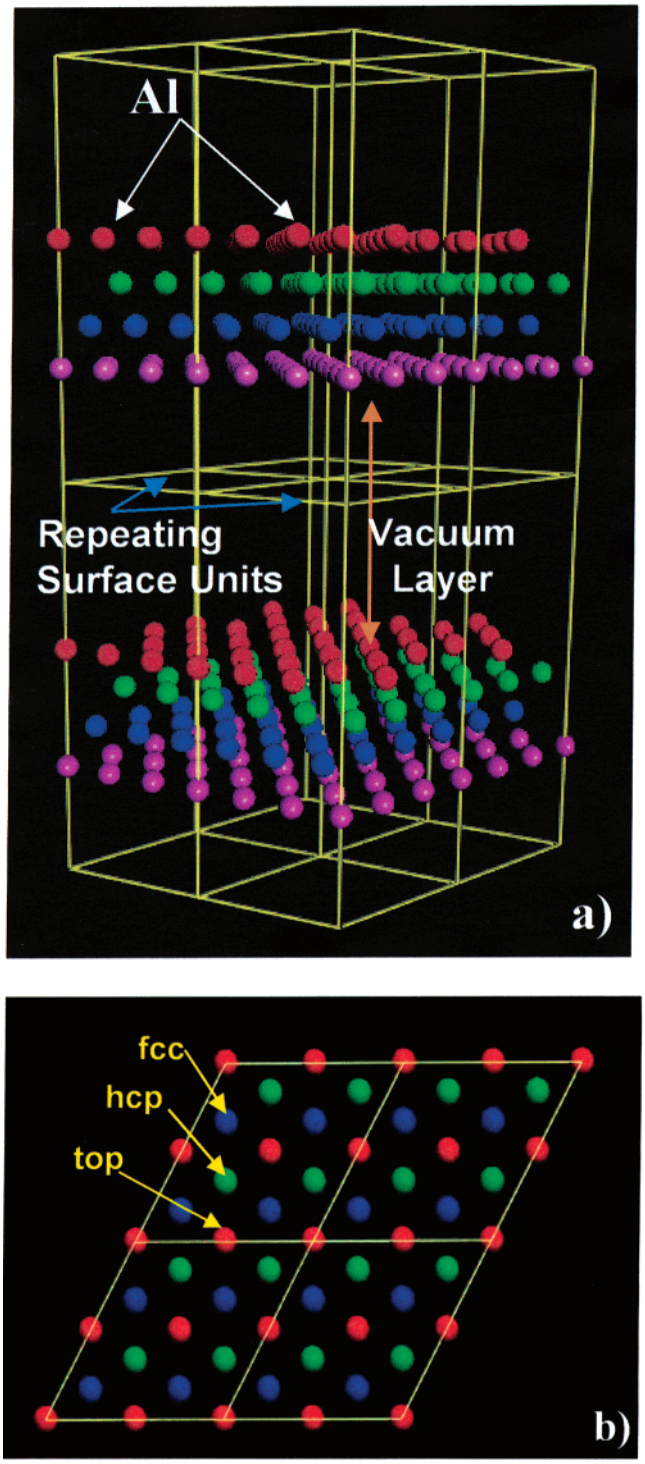

Figure 1. (a) Pictorial view of the aluminum slab model used in our calculations. Atoms in different layers are colored differently for easy identification of specific surface sites. Corresponding surface sites are depicted in panel b, which corresponds to a top view of the surface.

For the case of the FOX-7 molecule, we have shown in a previous study[19] that plane-wave DFT calculations using the VASP code provide an accurate description of the structural properties of this molecule and the corresponding crystal structure. The corresponding analysis will not be repeated here. The good agreement between our calculated properties of bulk aluminum and the isolated NM and FOX-7 molecules with the experiment and/or previous theoretical predictions made us confident to proceed to the next step: i.e., the investigation of molecular adsorption on the Al(111) surface.

B. Nitromethane Adsorption on Al(111) Surface. *B1. Geometries and Energies.* The adsorption of NM, which is a prototype for larger energetic molecules such as hexahydro-1,3,5-trinitro-*s*-triazine (RDX) or octahydro-1,3,5,7-tetranitro-1,3,5,7-tetrazocine (HMX), on the Al(111) surface was examined in detail for several distinct orientations of NM, relative to the metallic surface. For the case of nondissociative adsorption configurations, the corresponding adsorption energy (E_{ads}) was calculated according to the expression

$$E_{ads} = E_{molec} + E_{slab} - E_{(molec+slab)} \quad (1)$$

where E_{molec} is the energy of the isolated NM molecule in its equilibrium position, E_{slab} the total energy of the slab, and $E_{(molec+slab)}$ the total energy of the adsorbate/slab system. A positive E_{ads} value corresponds to a stable adsorbate/slab system. The energy of the isolated NM molecule for this calculation is that determined for the isolated NM molecule in a cubic cell with a dimension of 12 Å. The same Brillouin-zone sampling has been used to calculate the energies of the bare slab and of the molecule−slab systems.

Representative adsorption configurations are depicted in Figures 2 and 3. For each configuration, three views are represented. The first one, denoted with the index 1, represents the initial molecular configuration at the start of the optimization process. The second and third insets, denoted with indices 2 and 3, respectively, represent side and top views of the final adsorption configuration after full relaxation of the atomic positions.

In Figure 2, we present the adsorption configurations of NM when the C−N bond initially is oriented perpendicular to the surface, with the nitro group pointing down toward the surface. Panels a1−a3 illustrate the results obtained in which the adsorption of NM occurs at a face-centered cubic (fcc) site. In this case, various Al−O bonds are formed with equilibrium values of 1.897−2.098 Å. The final (i.e., optimized) configuration, denoted as NM(I) and represented in panels a2 and a3, illustrates marked distortions of the nitro group that are due to the strong interactions of the O and N atoms with the aluminum surface. As a result, the N−O bonds are significantly stretched to 1.455 and 1.476 Å, respectively, relative to the gas-phase equilibrium values of 1.240 Å. In addition, the nitro group and the C atom are no longer coplanar, as in the gas phase; however, in this state, the molecule adopts a chair conformation. The corresponding torsional angle τ(O−O−N−C) changes from the gas-phase value of 180° to −111.7° for this chemisorbed state. The large geometric changes that result upon adsorption are also reflected in a high adsorption energy. On the basis of eq 1 and the diagram level provided in Figure 4a, the predicted adsorption energy is $E_{Al+NM(I)} - E_{Al+NM(g)} = 43.3$ kcal/mol.

Panels b1−b3 of Figure 2 illustrate the case in which the initial configuration of the NM molecule interacts with an Al on-top site. As can be seen from the b2 and b3 images, adsorption at this site leads to complete dissociation of one of the O atoms from the nitro group. The dissociated O atom adsorbs at a nearby fcc site with simultaneous bonding to three neighboring Al atoms in the first layer. The corresponding Al−O bonds are almost identical, having values in the range of 1.85−1.86 Å. The remaining NM fragment, which is denoted as Ntr(I), also chemisorbs strongly to the surface, forming bonds to aluminum via both the N atom and the remaining O atom. The corresponding Al−N bond length is 1.849 Å, whereas the Al−O bond lengths are 1.896 and 1.904 Å. As in the case of the adsorption at the fcc site, the remaining (undissociated) N−O bond of the nitroso species is significantly stretched, with a length of 1.504 Å.

To determine the strength of the adsorption for this nitroso complex, we have used a relation similar to that given in eq 1, in which E_{slab} was taken as the energy of the slab and the dissociated O atom complex and E_{molec} was taken to be the energy of the isolated nitrosomethane species. The specific values of the energetic levels involved are shown in Figure 4a. Relative to the sum of energies of the surface with an adsorbed O atom and of the isolated nitrosomethane species (see $E_{Al+O(a)+Ntr(g)}$ in Figure 4a), the adsorbed nitroso complex at the fcc site ($E_{Al+O(a)+Ntr(\mathbf{I})}$) has an adsorption energy of $E_{Al+O(a)+Ntr(\mathbf{I})} - E_{Al+O(a)+Ntr(g)} = 127.6 - 60.5 = 67.1$ kcal/mol. This result indicates that, even after cleavage of the first N−O bond, the nitroso complex also interacts strongly with the aluminum surface.

Finally, we present, in panels c1−c3 of Figure 2, the results of adsorption at a hexagonal closely packed (hcp) surface site. In this case, both O atoms of the nitro group dissociate, which leads to the formation of a methylnitride chemisorbed species (denoted as MeN(I)). The dissociated O atoms occupy fcc surface sites and form strong bonds to the aluminum surface. The corresponding Al−O bonds have values of 1.847, 1.847, and 1.863 Å. The longest Al−O bonds correspond to those Al atoms that are also involved in simultaneous bonding to dissociated O atoms and the N atom of the methylnitride chemisorbed species (see panel c3 in Figure 2). Similarly, the N atom in the original nitro group also forms bonds to the metal surface, with Al−N bond lengths that vary over a range of 1.926−1.937 Å.

The strength of the interaction of methylnitride with the surface has been determined, with respect to the sum of energies of the surface with two adsorbed O atoms and that of isolated methylnitride chemisorbed species, as $E_{Al+2O(a)+MeN(\mathbf{I})} - E_{Al+2O(a)+MeN(g)}$. The corresponding energy levels are indicated in Figure 4a. On the basis of these values, we have determined the adsorption energy for methylnitride onto the surface to be 116.1 kcal/mol.

In addition to the vertical adsorption configurations previously described, we have also tested the case in which NM is initially oriented with the methyl group pointed toward the surface. In this case, chemisorption does not occur, because the methyl group does not interact with the surface Al atoms. Such configurations do not lead to stable adsorption configurations, and we have not investigated them further.

Beside the vertical adsorption configurations, we have also analyzed the case in which the NM molecule is initially oriented parallel to the metallic surface. We have examined three cases: the N atom of NM positioned above an Al surface atom (see panel a1 in Figure 3), above an hcp site (see panel b1 in Figure 3), and above an fcc site (see panel c1 in Figure 3). Our calculations indicate that, during the optimization of the atomic positions started from these parallel configurations, the NM molecule rotates, to maximize the interaction of the nitro group

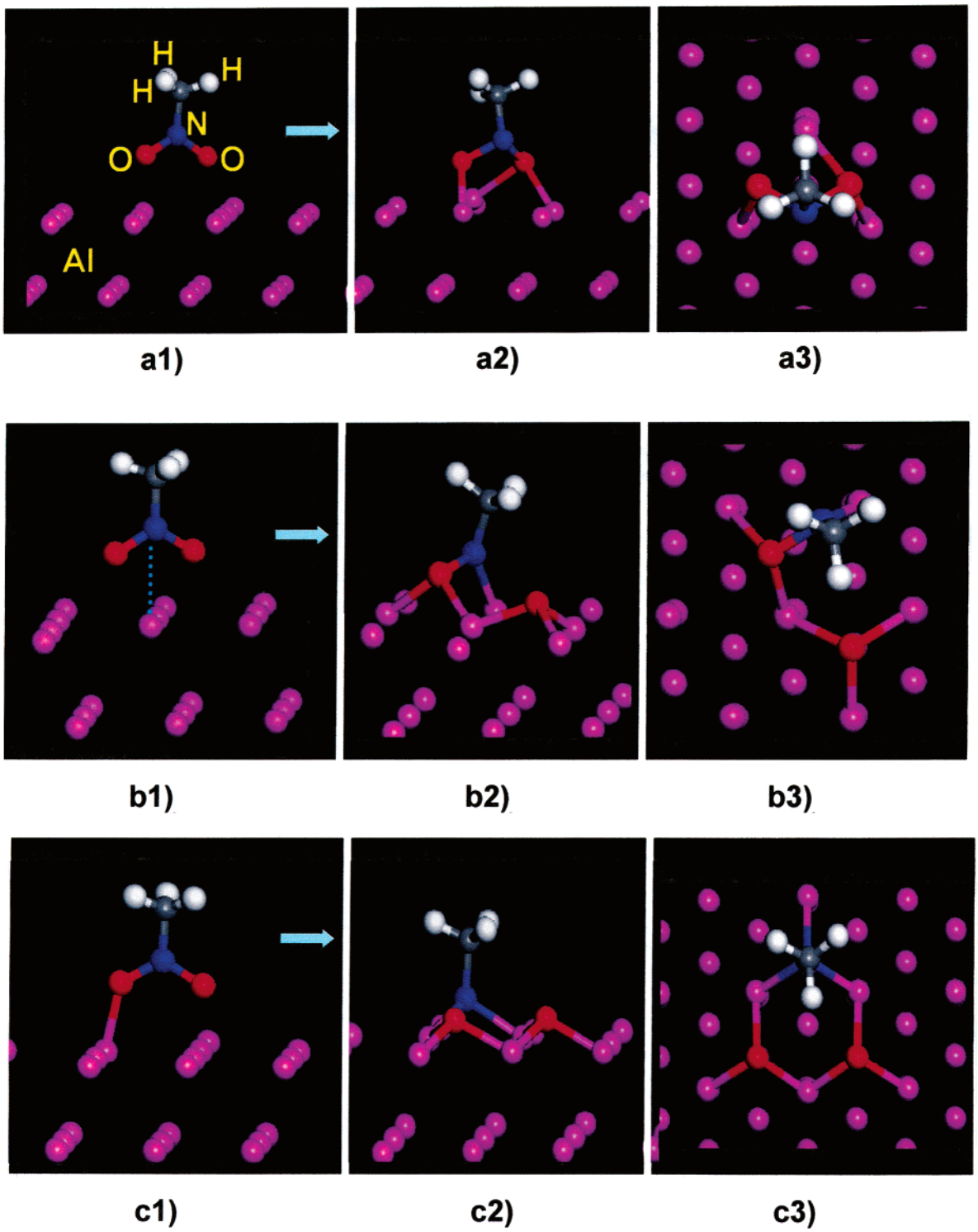

Figure 2. Adsorption configurations of NM on the Al(111) surface obtained from initial vertical configurations: (a) N atom above a fcc site (NM(I)), (b) N atom above an on-top site (Ntr(I)), and (c) N atom above an hcp site (MeN(I)). Initial configurations are depicted in panels a1−c1, whereas the lateral and top views of the corresponding final configurations are shown in panels a2−c2 and a3−c3, respectively.

with the aluminum surface. As a result, the molecule initially tilts such that the O atoms point toward the surface. In addition, depending on the particular molecular orientation, adsorption will occur either molecularly or dissociatively.

Panels a1−a3 of Figure 3 illustrate a case in which dissociation does notoccur, denoted as NM(**II**). In this case, rather large molecular deformations occur. As illustrated in panel a2 of Figure 3, the molecule adopts a chair configuration with a torsional angle of τ(O−O−N−C) = 115.6°. The molecular C−N axis is tilted by 28°, relative to the surface normal. As a result of intramolecular deformation, both the N and O atoms of the nitro group participate in the bonding to the aluminum surface. In this case, the Al−O bond lengths are 1.840 Å, whereas the Al−N bond length is 2.111 Å. The strong interaction with the metallic surface is also reflected by the stretched N−O bonds of the NM molecule, which are 1.429 Å long (0.19 Å larger than those in the gas-phase molecule). For the chemisorbed configuration with the N atom positioned above

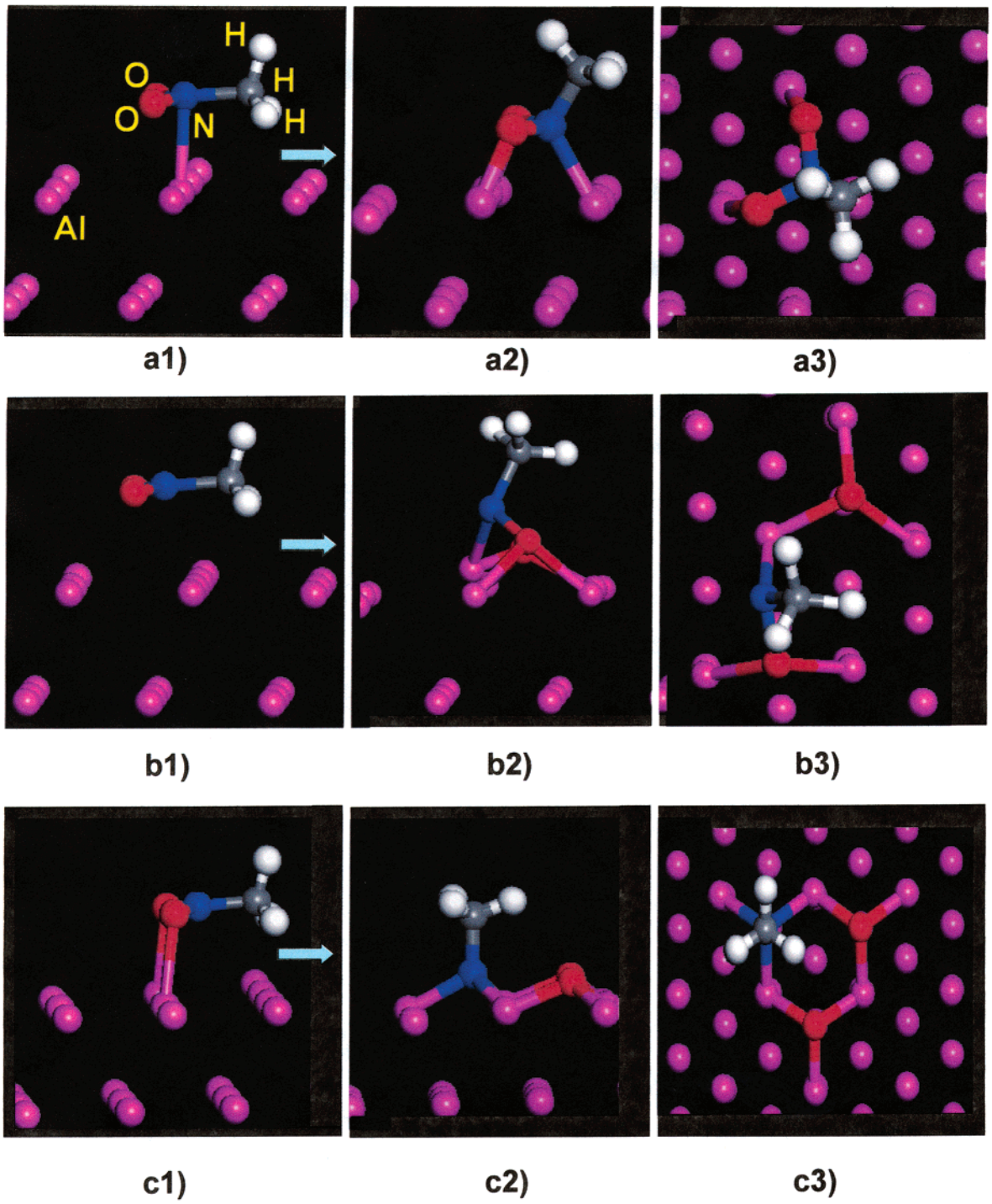

Figure 3. Adsorption configurations of NM on the Al(111) surface obtained from initial parallel configurations: (a) N atom above an on-top site (NM(II)), (b) N atom above an hcp site (Ntr(II)), and (c) N atom above a fcc site (MeN(II)). Initial configurations are depicted in panels a1−c1, whereas the lateral and top views of the corresponding final configurations are shown in panels a2−c2 and a3−c3, respectively.

an hcp site, we find a binding energy $E_{NM(II)}$ of 53.8 kcal/mol, which is slightly larger than that found for the undissociated state in which the optimization was started from a vertical configuration of NM ($E_{NM(II)}$).

In the case where the initial configuration corresponds to the N atom above an hcp site, adsorption on the aluminum surface leads to dissociation of one of the N−O bonds (see panels b2 and b3 of Figure 3), with the formation of chemisorbed nitrosomethane (denoted as Ntr(II)). The dissociated O atom is adsorbed at an fcc site and forms Al−O bonds with lengths in the range of 1.821−1.854 Å. The remaining O atom of the nitro group bonds to two surface Al atoms (r(Al−O) = 1.877 Å and 1.938 Å), whereas the N atom binds at a distance of 1.865 Å to an Al surface atom. As observed previously, an elongated N−O bond (1.523 Å) is observed. The corresponding binding energy of this nitrosomethane chemisorbed species is found to be $E_{(Al+O(a)+Ntr(II))} - E_{(Al+O(a)+Ntr(g))} = 60.1$ kcal/mol, which is similar to the value obtained for Ntr(I).

Finally, in the case where the N atom is initially positioned above an fcc site (panel c1 in Figure 3), adsorption leads to the dissociation of both O atoms. As a result, the O atoms form strong Al−O bonds (see panels c2 and c3 of Figure 3), whereas

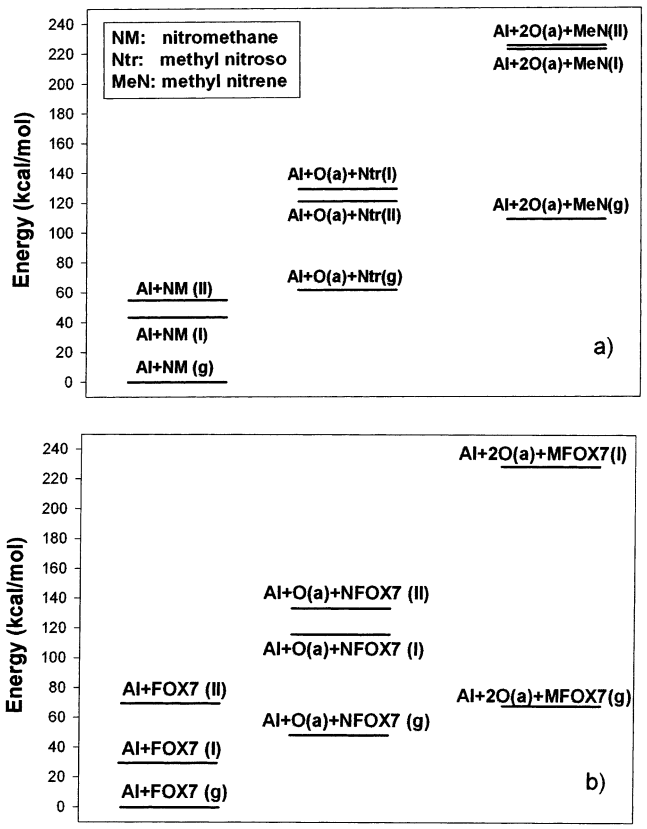

Figure 4. Relative energies of various configurations of (a) NM and (b) FOX-7 adsorbed on the Al(111) surface as described in text. Abbreviations used are as follows: (a), adsorbed configuration and (g), gas-phase configuration (the other abbreviations—NM(I), NM(II), Ntr(I), Ntr(II), MeN(I), MeN(II), FOX7(I), FOX7(II), NFOX7(I), NFOX7(II), and MFOX7(I)—are described in the text).

the remaining methylnitride chemisorbed species, denoted as MeN(II), adsorbs perpendicular to the surface (see panel c2 of Figure 3). It is important to note that the methylnitride chemisorbed species also binds strongly to the surface. On the basis of the energy values represented in Figure 4, we have obtained a value of 116.2 kcal/mol for the adsorption energy of the methylnitride chemisorbed species. This radical is bonded to the surface with Al−N bond lengths of 1.924, 1.936, and 1.936 Å.

Overall, these results indicate that NM can undergo both molecular and dissociative adsorption when deposited on the Al(111) surface. The fact that dissociation of the nitro group on the aluminum surface is observed in our simple energy minimizations suggests that the activation energies of these processes are minimal. Moreover, we note that, in addition to the formation of strong Al−O bonds, the dissociation products nitrosomethane or methylnitride also strongly bind to the surface through interactions of either N or O atoms.

B.2. Electron Localization Function and Charge Distribution. A useful tool to investigate the nature of the chemical interaction of NM with the Al(111) surface is the electron localization function (ELF), which is defined as[21,22]

$$\mathrm{ELF}(r) = \frac{1}{1 + \left(\frac{D(r)}{D_h(r)}\right)^2} \qquad (2)$$

where $D(r)$ is the Pauli excess kinetic energy density, defined as the difference between the kinetic energy density and the von Weizsäcker kinetic energy functional:

$$D(r) = \frac{\hbar^2}{2m}\nabla_r\nabla_{r'}\cdot\rho(\vec{r},\vec{r}') - \frac{1}{4}\left(\frac{\hbar^2}{2m}\right)\left(\frac{|\nabla\rho(\vec{r})|^2}{\rho(\vec{r})}\right) \qquad (3)$$

and $D_h(r)$ is the kinetic energy of the homogeneous electron gas for a density equal to the local density:

$$D_h(r) = \frac{3}{5}\frac{\hbar^2}{2m}(3\pi^2)^{2/3}\rho(r)^{5/3} \qquad (4)$$

with $\rho(r) = \sum_i|\varphi_i(r)|^2$ and $\varphi_i(r)$ being the Kohn−Sham orbitals.

The ELF function allows identification of regions of space having a high concentration of paired and unpaired electrons. The local maxima of the ELF are also called localization attractors.[21,22] The ELF value is 0.5 for a homogeneous electron gas and increases toward unity for electrons that are paired in a covalent bond or in the case of localized unpaired electrons in a dangling bond.

Isosurfaces of ELF can be calculated and used to help explain the bonding structure and charge localization in a chemical system. A plot of the isosurface for a constant value of ELF = 0.7 in the case of an isolated NM molecule is presented in Figure 5a. For this isosurface, several attractors can be observed in the figure: three corresponding to C−H bonds, one to the C−N bond, and two attractors on each O atom, corresponding to the lone-pair electrons. We notice that localization is strongest in the C−H bonds and in the lone electron pairs. Figure 5 illustrates the ELF isosurfaces corresponding to adsorption configurations of NM presented in Figure 2, namely the nondissociated state (NM(I), Figure 5b), the state with one O atom dissociated (Ntr(I), Figure 5c), and finally the state with both O atoms dissociated (MeN(I), Figure 5d).

For the nondissociative adsorption configuration (Figure 5b), we observe that the ELF distributions on O atoms change to ring shapes, corresponding to the formation of bonds to Al atoms. Also, a new attractor is present on the N atom, indicating new bonds to the substrate. In the case of the configuration with one dissociated O atom (Figure 5c), major changes are observed for the dissociated O and N atoms. In this case, there is localization of a small charge on the dissociated O atom. This indicates an ionic type of bonding. In addition, the charge localization on the N atom increases, relative to the nondissociated configuration, as indicated by the larger kidney shape attracted around this atom. Finally, in the case when both O atoms of NM dissociate, three different attractors are present around the N atom (see Figure 5d). These attractors have lobes that are directed toward the neighboring Al atoms. This corresponds to the formation of new bonds between the methylnitride and the surface.

A common tool to provide a semiquantitiative measure of charge transfer is the Mulliken population analysis[23] method, in which the electronic charge is partitioned among the individual atoms. This partitioning has been done using the formalism developed by Segall et al.[24] in the context of plane-wave calculations, as implemented in the CASTEP[25] package. Selective variations of the individual atomic Mulliken charges on O and N atoms of NM are presented in Figure 6a for the case of the isolated molecule (configuration 1), as well as for the three adsorbed states, namely the nondissociated state (configuration 2), the state with one O atom dissociated (configuration 3), and the state with both O atoms dissociated (configuration 4), as depicted in Figure 2 in panels a2, b2, and c2, respectively. The results of these calculations indicate that significant charge transfer occurs as a result of adsorption. In

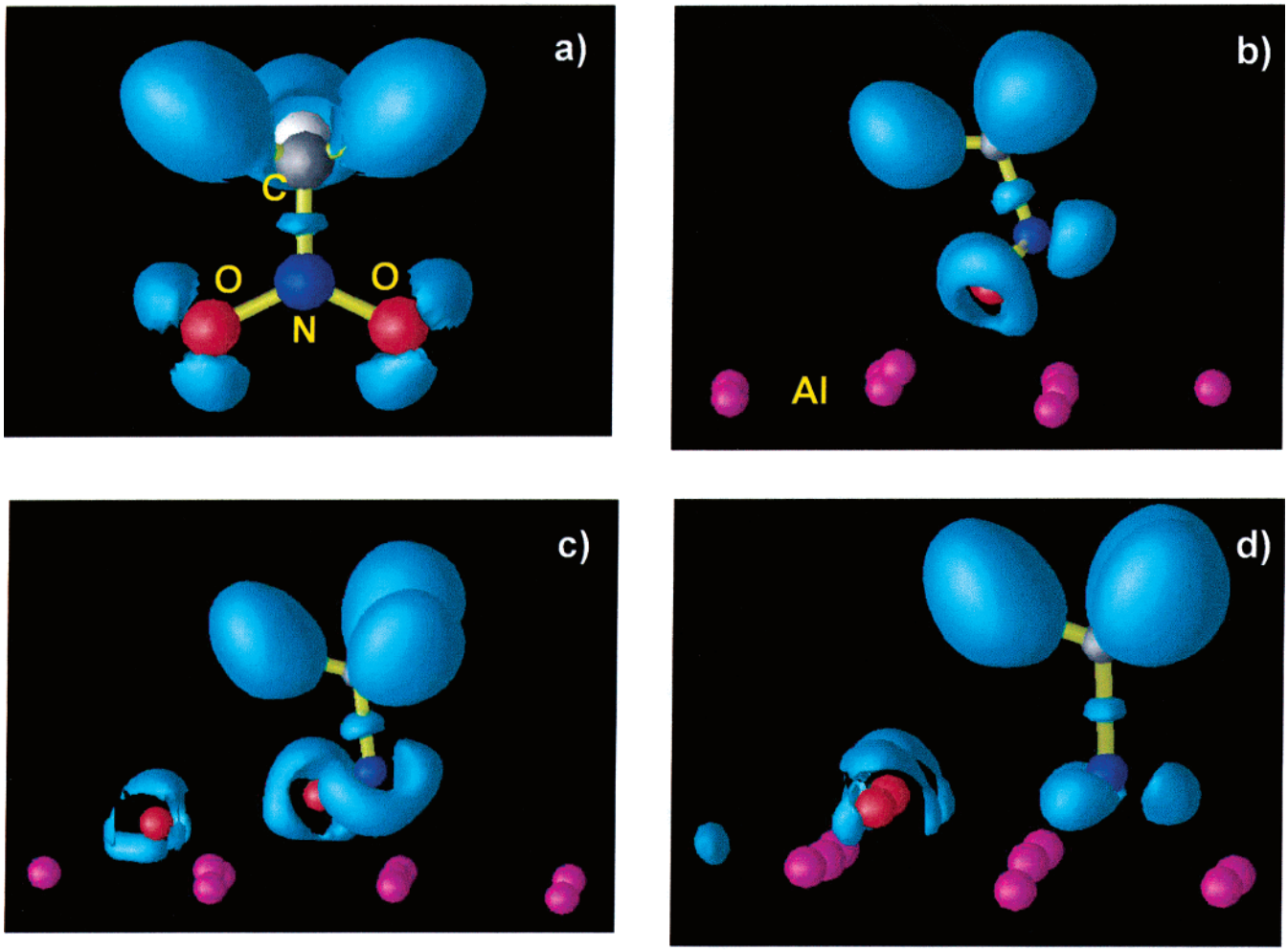

Figure 5. Comparison of the isosurfaces of the electron localization function (ELF = 0.7) for (a) NM in the gas phase, (b) NM molecularly adsorbed (NM(I)), (c) NM dissociatively adsorbed with one O atom dissociated (Ntr(I)), and (d) NM dissociatively adsorbed with both O atoms dissociated (MeN(I)). Configurations b, c, and d respectively correspond to structures a2, b2, and c2 shown in Figure 2.

the case of nondissociative adsorption, there is a significant increase in the negative charge of the O atoms, from −0.35 e to −0.63 e, relative to gas-phase NM case. A corresponding electron acceptance is observed for the N atom, whose charge decreases from 0.41 e to −0.02 e. Corresponding to this transfer of electrons to the NM molecule, there is an increase in the positive charge of the Al atoms that are bonded to the NM molecule, with values in the range of 0.38−0.51 e (not represented in Figure 6a).

The process of charge transfer also occurs for the case of dissociative adsorption. For example, in the case in which one O atom dissociates (see configuration c in Figure 5a) or both O atoms dissociate (see configuration d in Figure 5a), the Mulliken charges of these atoms decrease to a value of approximately −1 e. This is accompanied by a corresponding decrease of the charge on the N atom, from 0.5 e for the nitroso complex to −1.0 e for the methylnitride case. Simultaneously, there is a significant increase in the positive charge on the Al atoms involved in the bonding with either O atoms or with Ntr or MeN radicals with values in the range of 0.5−0.88 e. For the Al atoms that are simultaneously bonded with two O atoms or with an O atom and an N atom, some larger charges, in the range of 0.80−0.88 e, are observed.

Overall, these results indicate that there is significant charge transfer from the metallic surface to the NM molecule and its radicals. Moreover, the amount of charge transferred increases as the molecular dissociation increases. These results are consistent with the increase of the binding energy for molecular NM and its decomposition fragments to the surface.

C. FOX-7 Adsorption on Al(111) Surface. *C.1. Geometries and Energies.* The strong interactions of the nitro group of NM with the aluminum surface are likely to be present for other molecular systems that contain this chemical group. To test this notion, we have analyzed the adsorption of another energetic molecule, namely FOX-7. This organic compound, which was synthesized relatively recently,[20] is characterized as a promising high-energy-density material with superior shock-sensitivity properties. As in the case of NM, we have determined representative adsorption configurations of FOX-7 on the Al(111) surface for both vertical and parallel configurations, as illustrated in Figures 7 and 8, respectively. In each case, we present both the initial molecular configuration at the start of the optimization process, as well as the final state obtained by full optimization of the atomic coordinates.

Figure 7 shows three such sets of configurations of FOX-7 interacting with the Al(111) surface. In panel a1, the approximately planar FOX-7 molecule is initially positioned with the C═C axis perpendicular to the surface. One of the O atoms of the nitro groups is positioned approximately on top of an Al atom, whereas the C atoms are positioned above an fcc surface site. An additional perpendicular configuration, with the C atoms of the FOX-7 molecule positioned above an hcp site, is shown

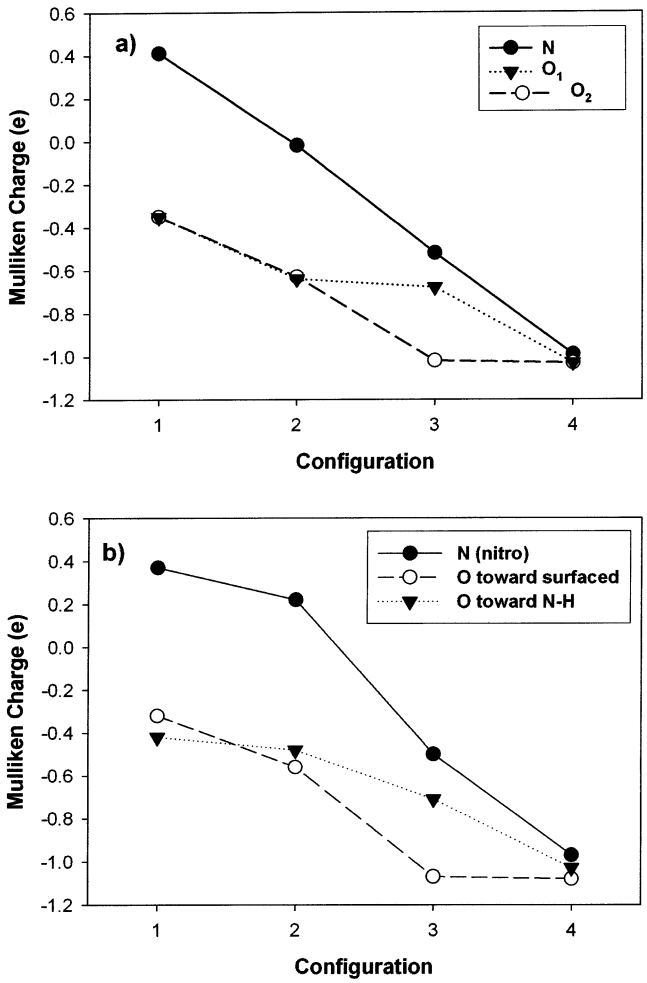

Figure 6. Variation of the Mulliken charges on the individual atoms of the nitro group for (a) NM and (b) FOX-7. In both cases, configuration 1 corresponds to gas-phase isolated molecules, whereas configurations 2, 3, and 4 correspond to the molecular adsorption state, the dissociative adsorption state with one O atom dissociated, and a dissociative adsorption state with both O atoms dissociated, respectively. These configurations correspond to those labeled as a2, b2, and c2 in Figure 2 for NM and as a2, b2, and c2 in Figure 7 for FOX-7, respectively.

in panel b1. Finally, in panel c1, the C═C molecular axis is tilted relative to the surface normal, such that both O atoms of the same nitro group interact with neighboring Al atoms.

From the results presented in panels a2 and a3 of Figure 7, we observe that adsorption occurs molecularly, with binding of one of the O atoms of each nitro group to an Al atom beneath it. We denote this configuration as FOX7(I). The Al−O distances are 1.868 Å. For this configuration, the major changes of the internal bonds are observed for the N−O bonds that are involved in bonding to the surface, which are stretched to ∼1.35 Å. In addition, the corresponding Al atoms where bonding occurs are raised upward, relative to the other surface atoms, by ∼0.33 Å. For this chemisorbed state (denoted as $E_{Al+FOX7(I)}$ in Figure 4b), the predicted binding energy is 28.4 kcal/mol. This value is smaller than that obtained for the undissociated molecular configuration of NM(I) (see panel a2 in Figure 2). This difference can be understood based on the number of direct bonds formed by the molecule to the surface. Indeed, we have noted that, in the case of NM, there is a significant deformation of the nitro group, which adopts a chair-type conformation such that both O and N atoms of the nitro group are involved in the bonding to the surface. For the FOX-7 molecule, however, only the O atoms participate in direct bonding, whereas the rest of the molecular structure does not undergo any significant deformation. The lack of deformation of the FOX-7 molecule may be due in part to the intramolecular N−H···O hydrogen bonds between the amino and nitro groups. These intramolecular interactions have a tendency to maintain the skeletal structure of the molecule.

In the case where adsorption is initiated in a vertical configuration with the C atom above an hcp site (see panel b1 in Figure 7), there is dissociative chemisorption of the FOX-7 molecule (see panels b2 and b3 in Figure 7), leading to oxygen abstraction by the surface Al atoms. The dissociated O atom binds to three neighboring Al atoms, with Al−O bond lengths in the range of 1.833−1.858 Å. The remaining nitroso-FOX-7 complex, denoted as NFOX7(I), tilts by 34°, relative to the surface normal, thus allowing the interaction of both nitro and nitroso groups with the surface. In this case, as can be seen in panel b3 of Figure 7, both the N and O atoms of the nitroso group interact simultaneously with one of the surface atoms, denoted as Al_1, forming bonds of lengths $r(N-Al_1) = 1.906$ Å and $r(O-Al_1) = 1.792$ Å. As a result of the strong interaction with the molecule, this surface Al_1 atom is pulled upward by a distance of 1.17 Å, relative to the surface plane. A similar upward displacement is observed for the other Al atom, denoted as Al_2, which is bonded to the undissociated nitro group. This atom is moved vertically by a distance of 0.81 Å.

A more quantitative measure of the interaction between the dissociated FOX-7 fragment and the Al(111) surface has been obtained by evaluation of the adsorption energy. Relative to the energy of the surface with an adsorbed O atom and that of the isolated nitroso-FOX-7 radical ($E_{Al+O(a)+NFOX7(g)}$), the adsorption energy is 69.1 kcal/mol. The calculated binding energy of this radical is similar to that of the nitroso complex (67.1 kcal/mol in the case of nitromethane adsorption). As in the NM case, we find that, after cleavage of the first N−O bond, the nitroso complex interacts strongly with the aluminum surface.

Finally, in the case when the initial configuration of the FOX-7 molecule is in a vertical plane but with the C═C axis tilted, relative to the surface normal, as illustrated in panel c1 of Figure 7, we observe that adsorption on the surface leads to dissociation of both O atoms of the same nitro group, with the formation of strong Al−O bonds. The remaining FOX-7 fragment is bonded to the surface through the N-atom end (r(N−Al) = 1.878 and 1.916 Å) and one O atom of the other nitro group (r(O−Al) = 1.853 Å). The Al atom (denoted as Al_1 in panel c2 in Figure 7) simultaneously bound to both N and O atoms of the FOX-7 fragment is displaced upward, relative to the surface plane, by a distance of 1.38 Å. For this FOX-7 radical (denoted as MFOX7(I)), we have estimated the value of the adsorption energy to be 160 kcal/mol. This binding energy is higher than that obtained in the case of the methylnitride chemisorbed species (116.1 kcal/mol). The increase in binding can be understood based on the increase in the number of direct bonds formed between the FOX-7 radical and the surface. Indeed, as illustrated in panel c2 of Figure 7, the FOX-7 radical is bonded to the surface through both the N atom of the dissociated nitro group as well as through one of the O atoms of the other undissociated nitro group. In the methylnitride case, the bonding was only through the N atom.

In Figure 8, we present the results of atomic optimizations when the FOX-7 molecule is initially placed in a plane parallel to the surface. Two configurations have been considered: first, (see panel a1 in Figure 8) one O atom of a nitro group interacts initially with a single Al atom of the surface; second, (see panel

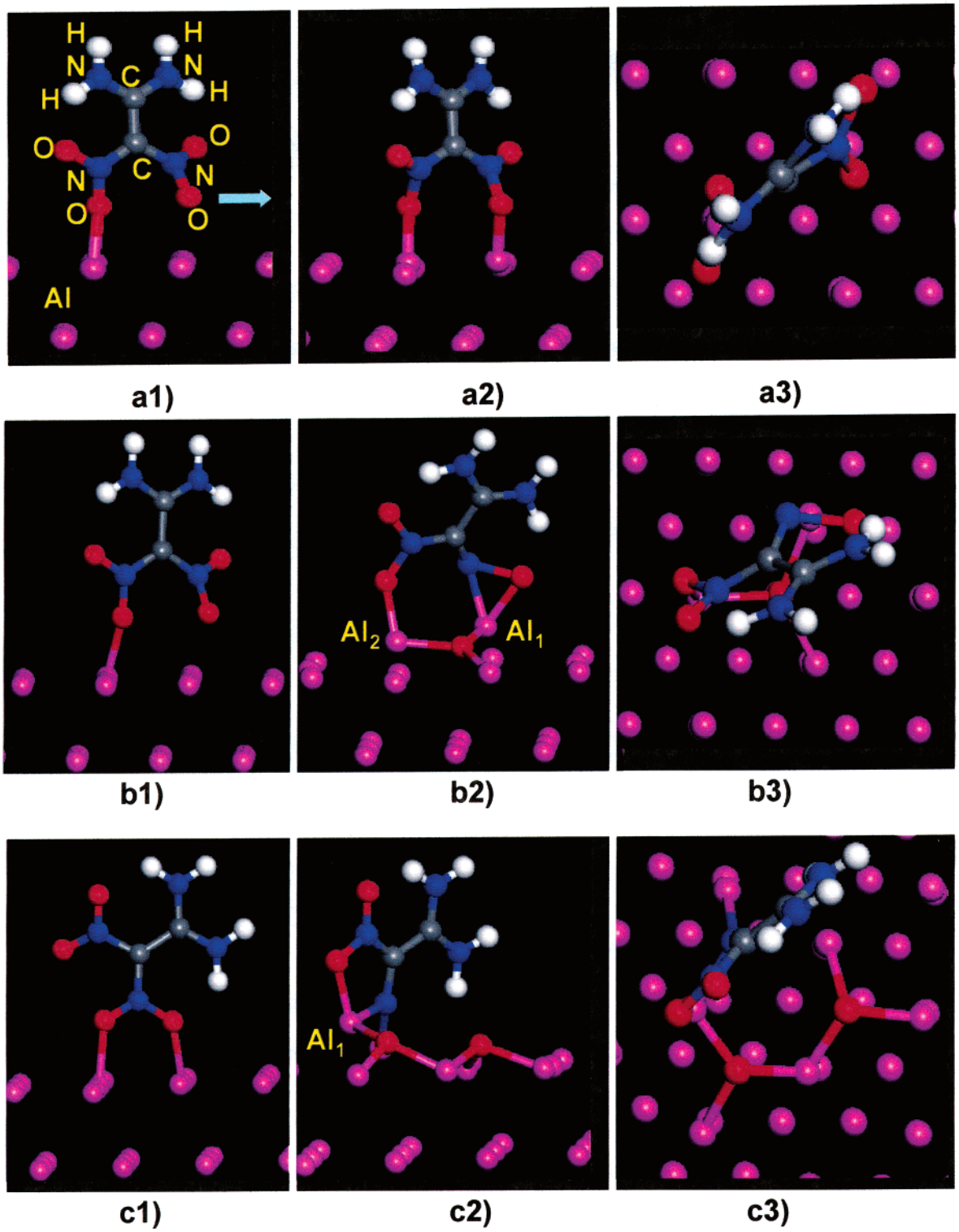

Figure 7. Adsorption configurations of FOX-7 on the Al(111) surface obtained from initial vertical configurations: (a) C atom above a fcc site (FOX7(I)), (b) C atom above an hcp site (NFOX7(I)), and (c) N atom above an hcp site (MFOX7(I)). Initial configurations are depicted in panels a1−c1, whereas the lateral and top views of the corresponding final configurations are presented in panels a2−c2 and a3−c3, respectively.

b1 in Figure 8) an O atom of a nitro group interacts simultaneously with two neighboring Al surface atoms. As in the case of NM adsorption that has been started from a parallel configuration, the FOX-7 molecule first rotates to maximize the interaction of the nitro groups to the surface. Then, depending on the particular molecular orientation, adsorption occurs either molecularly (see panels a2 and a3 in Figure 8) or dissociatively (see panels b2 and b3 in Figure 8).

For the first case, shown in panels a2 and a3 of Figure 8, which is denoted as FOX7(II), the C═C bond is tilted by ∼60°, relative to the normal to the surface, and all four O atoms bind independently to the surface, with Al−O bond lengths in the range of 1.83−1.84 Å. In addition, the C atoms that are bonded to the two nitro groups form a puckered structure (see panel a3 in Figure 8) with torsional angles τ(O−O−N−C) in the range of 118°−122°. The values of the same angles for the gas-phase

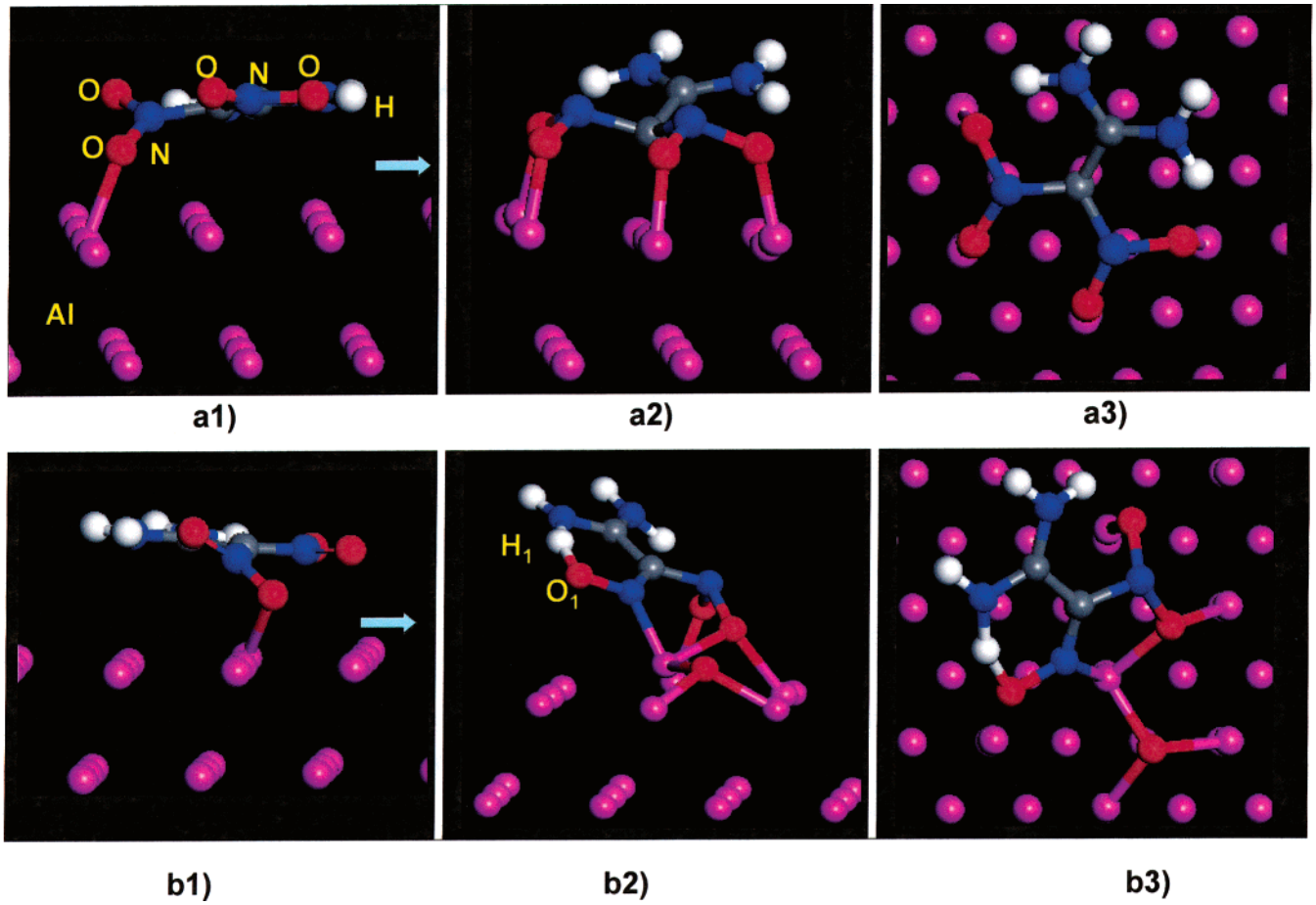

Figure 8. Adsorption configurations of FOX-7 on the Al(111) surface obtained from initial parallel configurations: (a) O atom interacts with a single Al atom (FOX7(II)) and (b) O atom interacts simultaneously with two Al atoms (MFOX7(II)). Initial configurations are depicted in panels a1 and b1, whereas the lateral and top views of the corresponding final configurations are presented in panels a2 and b2 and a3 and b3, respectively.

structure are ∼178°. The adsorption energy of this configuration is 69.5 kcal/mol. The increase in the binding energy, relative to the vertical configuration described earlier (see panel a2 in Figure 7), is clearly due to the fact that now there are four Al−O bonds instead of two bonds as observed previously.

Finally, adsorption initiated from a parallel configuration with simultaneous bonding of one of the O atoms to several Al surface atoms results in dissociation of the corresponding N−O bond (see panels b2 and b3 of Figure 8). The FOX-7 radical, which is denoted as NFOX7(II), again tilts, relative to the surface plane, such that the C═C bond makes an angle of ∼57° with the surface normal. The dissociated O atom binds to three Al surface atoms while the other O atom (denoted as O_1 in panel b2 of Figure 8) of the nitro group is significantly pulled toward the H atom of the amino group (denoted as H_1 in the same figure). As a result, the corresponding intramolecular hydrogen bond distance, r(O−H), decreases significantly from the gas-phase value of 1.738 Å to a value of 1.263 Å. The binding energy of this FOX-7 radical is 84.9 kcal/mol.

As in the case of NM, adsorption of FOX-7 on the Al(111) surface can lead to both molecular and dissociative configurations. For the dissociative cases, the O atoms of the nitro group become embedded into the surface and form strong Al−O bonds. In addition, FOX-7 fragments bond strongly to the surface through either N or O atoms.

C.2. Electron Localization Function and Charge Distribution. A comparison of the changes in the ELF isosurfaces for gas-phase FOX-7 and for various adsorption configurations is presented in Figure 9. For the isolated FOX-7 molecule (see Figure 9a), several attractors can be identified. For example, the attractors that correspond to C═C, C−N, and N−H bonds are clearly evident in this figure. In addition, the attractors that correspond to the lone pairs of electrons on the N atoms of the amino groups and on the O atoms of the nitro groups are also present. In panels b−d in Figure 9, we also illustrate the ELF isosurfaces that correspond to the adsorption configurations of FOX-7 that are shown in Figure 7, namely, the molecular state (Figure 9b), the state with one O atom dissociated (Figure 9c), and the state with both O atoms dissociated (Figure 9d).

As in the case of molecular adsorption of NM, the molecular adsorption of FOX-7 induces significant changes in the charge distributions on the O atoms. In this case, the kidney-shaped distribution that is observed in the gas phase on O atoms changes to a ring shape, corresponding to the formation of bonds to the Al atoms. In the case of the configuration with one dissociated O atom (Figure 9c), the most-pronounced changes in the charge distribution are observed for the case of the O and N atoms involved in dissociation. There is little localization of charge on the dissociated O atom, which is indicative of ionic bonding. However, charge localization on the N atom of the nitro group where dissociation occurs increases significantly, such that, now, a new attractor is present on this atom (see Figure 9c). Finally, in the case where both O atoms of FOX-7 dissociate, two different attractors are now present around the N atom, as shown in Figure 9d. These lobes are directed toward the two neighboring Al atoms and correspond to the formation of new bonds between the FOX-7 radical and the metallic surface.

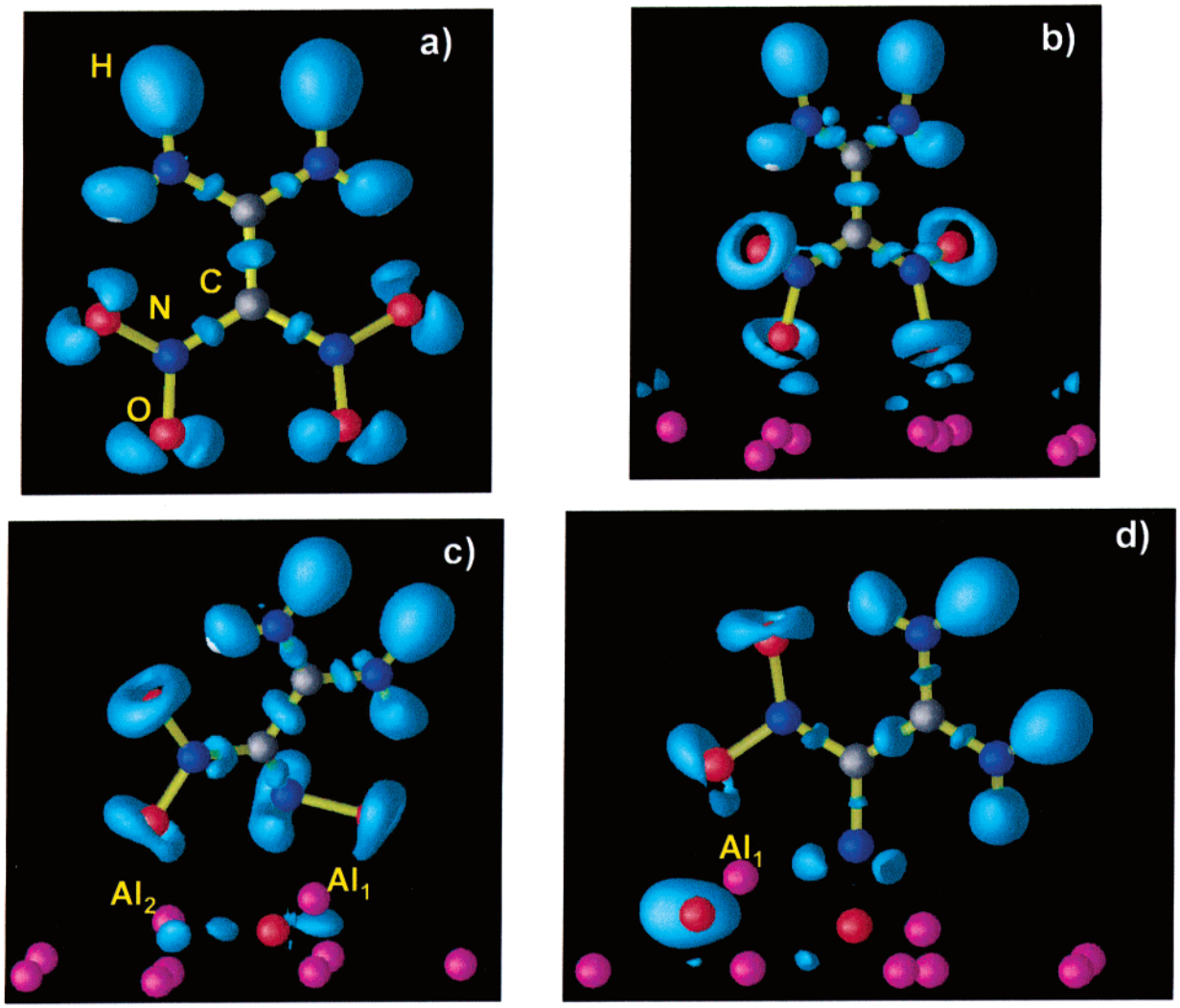

Figure 9. Comparison of the isosurfaces of the electron localization function (ELF = 0.7) for (a) FOX-7 in the gas phase, (b) FOX-7 molecularly adsorbed (FOX7(I)), (c) FOX-7 dissociatively adsorbed with one O atom dissociated (NFOX7(I)), and (d) FOX-7 dissociatively adsorbed with both O atoms dissociated (MFOX7(I)). Configurations b, c, and d respectively correspond to structures a2, b2, and c2 presented in Figure 7.

As in the case of NM adsorption, the most important charge variations occur on the nitro group of the FOX-7 molecule that is involved in direct bonding to the surface. The corresponding variation of the Mulliken charges on the corresponding to the N and O atom are presented in Figure 6b. Here, we have considered the case of the isolated molecule (configuration 1 in Figure 6b), as well as the three adsorbed states (namely, the nondissociated state (configuration 2), the state with one O atom dissociated (configuration 3), and the state with both O atoms dissociated (configuration 4), depicted in Figure 7 as panels a2, b2, and c2, respectively). The overall trend of the charge redistributions observed for the FOX-7 molecule is similar to that observed for NM (see Figure 6a). Namely, as a result of either molecular or dissociative adsorption on the surface, there is a significant electronic charge transfer from the surface to the molecule. The amount of charge transferred increases in the following order: molecular adsorbed state (configuration 2) → dissociative state with one dissociated O atom (configuration 3) → dissociative state with both O atoms dissociated (configuration 4). As shown in Figure 6b, there is a continuous decrease of the charges on both N and O atoms when going from configuration 2 to configuration 4. In the case of configuration 4 of Figure 6b, the charges on dissociated O atoms, as well as on the N atom of the nitro group involved in dissociation, are approximately −1 e. Corresponding to this transfer of electrons to the FOX-7 molecule, there is a corresponding increase in the positive charge of the Al atoms bonded either to the dissociated O atoms or to the remaining FOX-7 fragment. For example, the Al atoms bonded with a single O atom have charges in the range of 0.38−0.46 e. This positive charge increases to 0.94 e on the Al atoms that are bonded simultaneously with two O atoms. The largest charge increase is observed for those Al atoms that are bonded simultaneously to O and N atoms, namely atoms denoted as Al_1 in panels b2 and c2 in Figure 7. The corresponding charges on these atoms are 1.26 and 1.41 e, respectively. Overall, as in the case of NM, the increase in the amount of charge transferred to the adsorbed molecule or its dissociation fragments is directly correlated to the increase in the corresponding binding energy.

IV. Conclusions

The interactions of nitromethane (NM) and 1,1-diamino-2,2-dinitroethylene (FOX-7) molecules with the Al(111) surface have been investigated based on optimizations performed using spin-unrestricted generalized gradient approximation plane-wave density functional theory calculations. The main objective of this study was to determine the possible reaction mechanisms at the molecule−metallic-surface interface. The results of our calculations indicate a common propensity for oxidation of the

aluminum surface by the oxygen-rich nitro groups (NO_2) of the NM and FOX-7 molecules. Dissociation of the nitro groups and formation of strong Al−O bonds seems to be a common mechanism for these molecules. In addition, we have found that both the molecular adsorption and the dissociation processes occur with significant charge redistribution. These large charge redistributions have been found to be consistent with the strong binding energies for the dissociated O atoms and for the dissociation fragments of either NM or FOX-7 molecules. These results suggest that contact between nitro-containing energetic compounds and aluminum metal will result in rapid oxidation reactions.

Acknowledgment. The authors gratefully acknowledge grants of computer time at the Army Research Laboratory, Aeronautical Systems Center, and the Naval Oceanographic Office Major Shared Resource Centers, sponsored by the Department of Defense High Performance Computing Modernization Program. D.L.T. gratefully acknowledges support by the U.S. Army Research Office (under Grant No. DAAD 19-01-1-0503).

References and Notes

(1) Sutton, G. P. *Rocket Propulsion Elements*; Wiley: New York, 1992.

(2) Kwok, Q. S. M.; Fouchard, R. C.; Turcotte, A. M.; Lightfoot, P. D.; Bowes, R. *Propellants, Explos., Pyrotech*. **2002**, *27*, 229.

(3) Ivanov, G. V.; Tepper, F. In *Challenges in Propellants and Combustion 100 Years after Nobel*; Kuo, K. K., Ed.; Begell House: New York, 1997; p 636.

(4) See, e.g., Akhavan, J.; *The Chemistry of Explosives*; The Royal Society of Chemistry: Cambridge, U.K., 1998.

(5) Kresse, G.; Hafner, J. *Phys. Rev. B* **1993**, *B48*, 13115.

(6) Kresse, G.; Furthmüller, J. *Comput. Mater. Sci*. **1996**, *6*, 15.

(7) Kresse, G.; Furthmüller, J. *Phys. Rev. B* **1996**, *B54*, 11169.

(8) Vanderbilt, D. *Phys. Rev. B* **1990**, *B41*, 7892.

(9) Kresse, G.; Hafner, J. *J. Phys. Condens. Matter* **1994**, *6*, 824.

(10) Perdew, J. P.; Chevary, J. A.; Vosko, S. H.; Jackson, K. A.; Pedersen, M. R.; Singh, D. J.; Frolhais, C. *Phys. Rev. B* **1992**, *B46*, 6671.

(11) Monkhorst, H. J.; Pack, J. D. *Phys. Rev. B* **1976**, *B13*, 5188.

(12) Methfessel, M.; Paxton, A. T. *Phys. Rev. B* **1989**, *B40*, 3616.

(13) Kresse, G.; Hafner, J. *Phys. Rev. B* **1993**, *B47*, 588.

(14) Murnaghan, F. D. *Proc. Natl. Acad. Sci. U.S.A.* **1944**, *30*, 2344.

(15) King, H. W. In *CRC Handbook of Chemistry and Physics*, 81st ed.; Lide, D. R., Ed.; CRC Press: Boca Raton, FL, 2000.

(16) Gaudoin, R.; Foulkes, W. M. C. *Phys. Rev. B* **2002**, *B66*, 052104.

(17) Sorescu, D. C.; Rice, B. M.; Thompson, D. L. *J. Phys. Chem. B* **2000**, *104*, 8406.

(18) Lide, D. R., Ed.; *CRC Handbook of Chemistry and Physics*, 81st ed.; CRC Press: Boca Raton, FL, 2000; Section 9.

(19) Sorescu, D. C.; Boatz, J. A.; Thompson, D. L. *J. Phys. Chem. A* **2001**, *105*, 5010.

(20) Latypov, N. V.; Bergman, J.; Langlet, A.; Wellmar, U.; Bemm, U. *Tetrahedron* **1998**, *54*, 11525.

(21) Silvi, A.; Savin, A. *Nature* **1994,** *371*, 683.

(22) Savin, A.; Nesper, R.; Wengert, S.; Fässler, T. F. *Angew. Chem., Int. Ed. Engl*. **1997**, *36*, 1808.

(23) Mulliken, R. S. *J. Chem. Phys*. **1955**, 23, 1833, 2343.

(24) Segall, M. D.; Pickard, C. J.; Shah, R.; Payne, M. C. *Phys. Rev. B* **1996**, *B54*, 16317.

(25) Milman, V.; Winkler, B.; White, J. A.; Pickard, C. J.; Payne, M. C.; Akhmatskaya, E. V.; Nobes, R. H. *Int. J. Quantum Chem*. **2000**, *77*, 895.